THE JOURNAL OF PHYSICAL CHEMISTRY A

Article

pubs.acs.org/JPCA

Photochemistry of Matrix Isolated (Trifluoromethyl)sulfonyl Azide, $CF_3SO_2N_3$

Xiaoqing Zeng,*[,†] Helmut Beckers,*[,‡] Helge Willner,[‡] Patrik Neuhaus,[§] Dirk Grote,[§] and Wolfram Sander[§]

[†]College of Chemistry, Chemical Engineering and Materials Science, Soochow University, 215123 Suzhou, China

[‡]FB C-Anorganische Chemie, Bergische Universität Wuppertal, Gaussstrasse 20, 42119 Wuppertal, Germany

[§]Lehrstuhl für Organische Chemie II, Ruhr-Universität Bochum, Universitätsstraß 150, 44780 Bochum, Germany

Supporting Information

ABSTRACT: The photochemistry of matrix isolated (trifluoromethylsulfonyl) azide, $CF_3SO_2N_3$, has been studied at low temperatures. Upon ArF laser irradiation (λ = 193 nm), the azide eliminates N_2 and furnishes triplet [(trifluoromethyl)sulfonyl]nitrene, CF_3SO_2N, which has been characterized by IR and EPR spectroscopy. Upon subsequent UV light irradiation (λ = 260−400 nm) the nitrene converts to $CF_3N{=}SO_2$ and $CF_3S(O)NO$ through a Curtius-type rearrangement. Further two new species $CF_2N{=}SO_2F$ and FSNO were identified together with CF_2NF, SO_2, F_2CO, CF_3NO, and SO as side products. In addition, triplet nitrene CF_3N was detected by its EPR and IR spectra. The complex stepwise photodecomposition of matrix isolated $CF_3SO_2N_3$ is discussed in terms of the observed photolysis products and quantum chemical calculations.

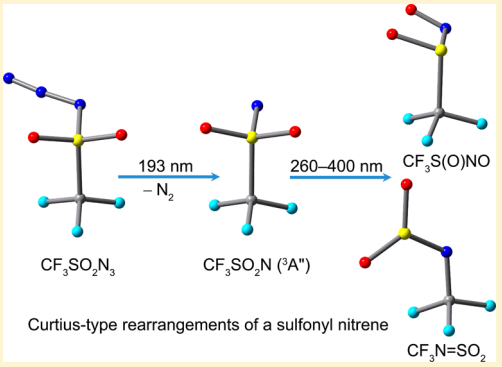

INTRODUCTION

Sulfonyl azides, RSO_2N_3, are important reagents in synthetic chemistry.[1−4] Similar to the reactions of related carbonyl azides,[5,6] both photodecomposition and thermal decomposition reactions of sulfonyl azides have been extensively studied in solution. The intervention of sulfonylnitrenes, RSO_2N, were chemically inferred from secondary decomposition products.[7−17] A number of triplet sulfonylnitrenes have already been experimentally detected among the photolysis products of the corresponding azides by electron paramagnetic resonance (EPR) spectroscopy at low temperatures.[18−20] These early studies strongly suggested that sulfonylnitrenes adopt triplet ground states, and no straightforward evidence for a Curtius-type rearrangement was obtained.

Recently, laser flash photolysis of arylsulfonyl azide was studied by ultrafast absorption spectroscopy (IR and UV−vis).[21,22] The (2-naphthylsulfonyl)nitrene intermediate (2-$NpSO_2N$) has been verified to be formed in both the singlet and the triplet states, whereas the rather short-lived (τ = 700 ± 300 ps in CCl_4) singlet nitrene was found to relax to the long-lived triplet ground state. Still no conclusive evidence have been established for a Curtius-type rearrangement of 2-$NpSO_2N$.[21] The complex photochemistry in solution and the congested spectra of the photolysis products prevented as yet an unambiguous detection of the potential rearrangement product 2-$NpNSO_2$.

In comparison to the complex photochemistry in solution, photolysis of the facile sulfonyl azide FSO_2N_3 in solid noble gas matrices was found to be much simpler.[23] Upon ArF excimer laser photolysis (193 nm), triplet nitrene FSO_2N was obtained and characterized by IR, UV−vis, and EPR spectroscopy. In addition to the minor side products SO + FNO and FN + SO_2, the oxygen-shifted Curtius-type rearrangement product FS(O)-NO was identified after subsequent irradiation with light of λ > 320 nm. A similar rearrangement has been verified for the related α-oxo nitrene $F_2P(O)N \rightarrow F_2PNO$.[24] The first unambiguous spectroscopic proof for the expected Curtius-type rearrangement from RSO_2N to a sulfuryl imide $RN{=}SO_2$ was achieved for FSO_2N (R = F).[25] Traces of $FN{=}SO_2$ were identified among the photolysis (λ = 266 nm) products of FSO_2N,[25] which was synthesized in a high-yield (∼70%) by flash pyrolysis of FSO_2N_3. In contrast, no Curtius-type rearrangement product was found among the pyrolysis products of FSO_2N_3, and also the previously studied flash pyrolysis of $CF_3SO_2N_3$ revealed very different results. No sulfonylnitrene CF_3SO_2N but O_2SN and CF_3 were obtained as main decomposition products.[26]

The rich and diverse chemistry of sulfonyl azides prompted us to study the photodecomposition of the broadly used diazo transfer reagent (trifluoromethyl)sulfonyl azide, $CF_3SO_2N_3$,[27] in solid noble gas matrices by IR and EPR spectroscopy. The stepwise decomposition of the azide to form CF_3NSO_2 and

Special Issue: Markku Rasanen Festschrift

Received: June 23, 2014
Revised: July 24, 2014

   dx.doi.org/10.1021/jp506243s | J. Phys. Chem. A XXXX, XXX, XXX−XXX

$CF_3S(O)NO$ via the nitrene CF_3SO_2N will be discussed, aided by DFT calculations.

EXPERIMENTAL SECTION

Sample Preparation. (Trifluoromethyl)sulfonyl azide, $CF_3SO_2N_3$, was prepared by treatment of $(CF_3SO_2)_2O$ with NaN_3 according to the known protocol.[28] For the preparation of ^{15}N-labeled $CF_3SO_2N_3$, sodium [1-^{15}N]azide (98 atom % ^{15}N, EURISO-TOP GmbH) was used. Before use, the quality of the substances was checked by gas-phase IR spectroscopy. A sample of CF_3N_3 was taken from our stock stored in a long-term Dewar vessel.

Matrix IR Spectroscopy. Matrix IR spectra were recorded on a FT-IR spectrometer in reflectance mode using a transfer optic. A KBr beam splitter and an MCT detector were used in the region 4000−550 cm^{-1}. A Ge-coated 6 μm Mylar beam splitter combined with a He(l)-cooled Si bolometer and a CsI window at the cryostat were used in the region 700−180 cm^{-1}. For each spectrum, 200 scans at a resolution of 0.25 cm^{-1} were coadded. The gaseous samples were mixed with noble gas (argon or neon, 1:1000) in a 1 L stainless-steel storage container, and then small amounts (ca. 1 mmol) of the mixture were deposited within 30 min onto the cold matrix support (5 K for Ne, 16 K for Ar, Rh plated Cu block) in a high vacuum of about 10^{-5} mbar. Photolysis experiments were carried out with an ArF excimer laser (Lambda-Physik, 2 mJ, 5 Hz) and by conducting the light of a high-pressure mercury lamp (TQ 150, Heraeus) through water-cooled quartz lenses combined with different cut off or interference filters (Schott). Details of the matrix apparatus have been described elsewhere.[29]

Matrix EPR Spectroscopy. For EPR measurements, the matrices were deposited on an oxygen-free high-conductivity copper rod (75 mm in length, 3 mm in diameter) that was cooled by a Sumitomo SHI-4-5 closed-cycle 4 K cryostat. The vacuum system consisted of a vacuum shroud equipped with a sample inlet valve and a quartz tube (75 mm length, 10 mm diameter) half-closed at the bottom. The vacuum pump system consists of a Pfeiffer Vacuum TMU071P turbo pump backed by a Leybold two-stage, rotary-vane pump. During deposition, the inlet port was positioned at the same height as the tip of the copper rod, and for the measurement of the EPR spectra the whole apparatus was moved downward so that the quartz tube and copper rod were positioned inside the EPR cavity. X-band EPR spectra were recorded with a Bruker Elexsys E500 ESR spectrometer equipped with an ER077R magnet (75 mm pole cap distance) and an ER047 XG-T microwave bridge. Computer simulation of EPR spectra were performed using the XSOPHE computer simulation software suite (version 1.0.4),[30] developed by the Centre for Magnetic Resonance and Department of Mathematics, University of Queensland, Brisbane (Australia), and Bruker Analytik GmbH, Rheinstetten (Germany).

Computational Details. Geometry optimizations were performed using DFT methods (B3LYP,[31] MPW1PW91,[32] BP86[33]) combined with the 6-311+G(3df) basis. The complete basis set method CBS-QB3[34] was used for energy calculation. Time-dependent (TD) DFT (B3LYP/6-311+G(3df)) calculations[35,36] were performed for the prediction of UV−vis transitions. Local minima were confirmed by vibrational frequency analysis, and transition states were further confirmed by intrinsic reaction coordinate (IRC) calculations.[37,38] All the calculations were performed using the Gaussian 03 software package.[39]

RESULTS AND DISCUSSION

Matrix Isolation Spectroscopy. (Trifluoromethyl)-sulfonyl azide exhibits a strong UV absorption band at about 193 nm, thus ArF laser irradiation was applied to study the photodecomposition of the Ne-matrix isolated sample at 6 K. Efficient depletion of the azide with concomitant formation of new species was observed, and the IR difference spectrum in the mid-infrared region is depicted in Figure 1. Bands with high

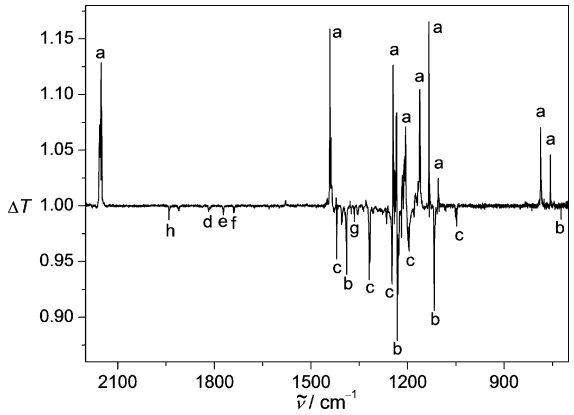

Figure 1. IR spectral changes (transmission T) in the region 2200−700 cm^{-1} obtained upon ArF laser photolysis (193 nm, 5 min) of Ne-matrix isolated $CF_3SO_2N_3$ (a) at 6 K. Assigned photolysis products: CF_3SO_2N (b), CF_3NSO_2 (c), $CF_3S(O)NO$ (d), CF_2NSO_2F (e), CF_2NF (f), SO_2 (g), and F_2CO (h).

frequencies at 1941.1 and 1911.8 cm^{-1} are assigned to F_2CO (h) by comparison with its known IR spectrum in Ne-matrix (1940.6 and 1911.6 cm^{-1}).[40] Weak bands of SO_2 (g) at 1355.2 and 1147.9 cm^{-1} can also be identified by reference to its IR spectrum in Ne-matrix (1356.1 and 1148.0 cm^{-1}).[23] However, the assignment of the new bands is not straightforward due to the congested spectrum in the region of 1400−1100 cm^{-1}, where the stretching vibrations of the CF_3 and SO_2 moieties are expected.

For further assignments, photolysis experiments were carried out in solid argon matrices at 16 K using a ^{15}N-labeled azide sample ($CF_3SO_2{}^{15}N_\alpha N_\beta N_\gamma$:$CF_3SO_2N_\alpha N_\beta{}^{15}N_\gamma$ = 1:1). The IR difference spectra are shown in Figure 2A,B, respectively. Compared to the Ne-matrix experiment results, the yields of the carriers d, e, and f in the spectral region 2000−1500 cm^{-1} are strongly enhanced, as well as the two IR bands labeled by j and i in Figure 2A. The ^{15}N-labeling experiment strongly facilitates the assignment, because all IR bands in this region except those of F_2CO (h) occur as doublets and reveal distinct isotope shifts. Among these IR bands, the weak one at 1593.5 cm^{-1} ($\Delta\nu(^{15/14}N)$ = 26.4 cm^{-1}) is assigned to CF_3NO (i) by referring to its known Ar-matrix spectrum (1593.4 cm^{-1}, $\Delta\nu(^{15/14}N)$ = 26.9 cm^{-1}).[41] Also $CF_2{=}NF$ (f, 1737.2 cm^{-1}, $\Delta\nu(^{15/14}N)$ = 16.7 cm^{-1}) is assigned by comparison to known gas-phase spectra (1740.3 cm^{-1}).[42]

The ArF laser photolysis products of $CF_3SO_2N_3$ were subsequently irradiated by using a high-pressure mercury lamp combined with an UV band-pass filter (Schott, UG11, λ = 260−400 nm). The corresponding IR difference spectra for the natural and ^{15}N-labeled samples are shown in Figure 2C,D, respectively. Upon irradiation, the IR bands of species (b) were depleted. Its band positions and isotopic shifts are summarized in Table 1. The experimental data are compared with calculated

dx.doi.org/10.1021/jp506243s | J. Phys. Chem. A XXXX, XXX, XXX−XXX

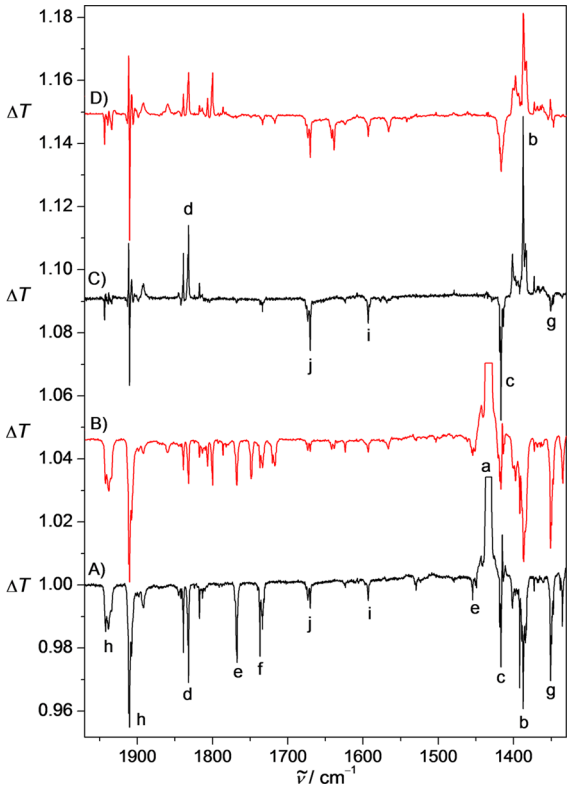

Figure 2. IR spectral changes (transmission T) in the region 1970−1330 cm^{-1} obtained upon ArF laser photolysis (193 nm, 10 min) of Ar-matrix isolated $CF_3SO_2N_3$ (a) at 16 K: (A) natural sample; (B) mixed $CF_3SO_2{}^{15}N_\alpha N_\beta N_\gamma$ and $CF_3SO_2N_\alpha N_\beta{}^{15}N_\gamma$ (1:1) sample. IR difference spectra (C) and (D) are obtained from (A) and (B), respectively, after subsequent UV irradiation (λ = 260−400 nm, 10 min). Assignments: CF_3SO_2N (b), CF_3NSO_2 (c), $CF_3S(O)NO$ (d), CF_2NSO_2F (e), CF_2NF (f), SO_2 (g), F_2CO (h), CF_3NO (i), and FSNO (j).

spectra (B3LYP/6-311+G(3df)) of CF_3SO_2N (b), the most likely candidate, in both the singlet and triplet states. The good agreement between the observed and calculated frequencies corroborates our assignment of several IR bands to triplet CF_3SO_2N (b, $^3A''$), which is further supported by our EPR spectroscopic studies (*vide infra*).

The identification of CF_3SO_2N (b) among the photolysis products enables a conclusive assignment of the IR bands (Table 2) of its photoinduced Curtius-rearrangement product $CF_3N{=}SO_2$ (c), which previously was suggested as one of the thermal decomposition products of $CF_3SO_2N_3$.[26] Therefore, it is clear that both photolytic and thermal decomposition of $CF_3SO_2N_3$ furnishes $CF_3N{=}SO_2$. This observation is in sharp contrast to the chemistry of FSO_2N_3, for which the main photoinduced decomposition route is an oxygen shift to yield FS(O)NO, whereas the sulfuryl imide $FN{=}SO_2$ was observed only as a minor product. Neither of these two compounds was found among the thermal decomposition products of FSO_2N_3.[25] Searching for $CF_3S(O)NO$, we find that DFT calculations (Table S1, Supporting Information) predict two close-in-energy conformers distinguishable by their characteristic N−O stretching vibrations at 1903 (*syn*-conformer) and 1847 cm^{-1} (*anti*-conformer). Indeed, a sharp band at 1832.3 cm^{-1} accompanied by a weaker matrix-site band at 1838.7 cm^{-1} (Figures 1 and 2A) can be safely assigned to *syn*-$CF_3S(O)NO$. This band shifts by 32.0 cm^{-1} upon ^{15}N-labeling (Figure 2B), in good agreement with the predicted value for *syn*-$CF_3S(O)NO$ ($\Delta\nu(^{14/15}N)_{syn}$ = 33.3 cm^{-1}). However, the expected medium strong IR bands of $CF_3S(O)NO$ (d) in the CF_3-stretching region (1200−1100 cm^{-1}) are blended by strong IR bands of other CF_3-bearing molecules.

According to Figure 2C, $CF_3S(O)NO$ (d) is depleted after UV irradiation (260−400 nm). In addition to traces of F_2CO (h) and CF_3NO (i), a new species (labeled by j in Figure 2) is formed, showing a N−O stretching vibration at 1670.5 cm^{-1} and an ^{15}N-isotopic shift of 32.0 cm^{-1}. Considering a monomolecular reaction in solid noble gas matrices, a mass balance for the decomposition of (d) to either F_2CO (h) or CF_3NO (i) requires the simultaneous formation of FSNO or SO, respectively. Indeed, both decomposition routes for $CF_3S(O)NO$ (d) are verified experimentally. A weak band at 1139.6 cm^{-1} proves the formation of SO (k, Figure 3), which appeared fairly close to its reported frequency at 1139.5 cm^{-1} observed in solid argon.[23] The nitroso derivative FSNO was found to be the global minimum of several possible isomers (FNSO, FSNO, FS(O)N) (Table S2, Supporting Information). The N−O stretch corresponds to the strongest IR band of FSNO, which is predicted at 1693 cm^{-1} with a ^{15}N-isotopic shift of 33.2 cm^{-1}. These values are in good agreement with the observation at 1670.5 cm^{-1} and $\Delta\nu(^{14/15}N)$ = 32.0 cm^{-1}. The observed N−O stretch of FSNO (1670.5 cm^{-1}) is close to but reasonably higher than those of CF_3SNO (1660 cm^{-1}, gas phase) and CH_3CH_2SNO (1530 cm^{-1}, gas phase),[43] which is in accord with the expected electron-withdrawing capabilities of the substituents. The predicted weaker F−S stretching band at 590 cm^{-1} of FSNO (j) could not be clearly assigned, probably due to its interference with the ν_6 band of CF_3SO_2N (b) at 553.2 cm^{-1}, for which several strong matrix sites appeared at 552.0 and 548.6 cm^{-1}.

A further proof of the photosensitivity of $CF_3S(O)NO$ (d) was found by the absence of this intermediate during the full-range high-pressure mercury lamp irradiation (λ > 225 nm) of Ar-matrix isolated $CF_3SO_2N_3$ (Figure 3). Time-dependent (TD) DFT calculations (Table S3, Supporting Information) predicted the existence of UV transitions near λ_{max} = 374 and 291 nm for $CF_3S(O)NO$ (d), which accounts for the observed depletion of this species under the filtered UV irradiation of λ = 260−400 nm (Figure 2C,D). The main products obtained after λ > 225 nm irradiation of Ar-matrix isolated $CF_3SO_2N_3$ (Figure 3) turned out to be $CF_3N{=}SO_2$ (c) and the fragment species CF_2NF (f) + SO_2 (g), F_2CO (h) + FSNO (j), and CF_3NO (i) + SO (k). The first pair of fragments may arise by photoinduced SO_2 elimination from $CF_3N{=}SO_2$ (c) followed by the known CF_3N (l) to CF_2NF (f) rearrangement.[44] The last pair of fragments is likely formed from $CF_3S(O)NO$ (d) by SO elimination, as proved by the photodecomposition of (d) shown in Figure 2C,D. The second pair of fragments (F_2CO + FSNO) cannot be formed by a simple elimination reaction. Nevertheless, the presence of a CF_2 group and a F−S bond in the fragments suggest that one fluorine atom in $CF_3N{=}SO_2$ (c) may have been shifted to the sulfur atom to yield $CF_2{=}NSO_2F$ (e), which subsequently decomposed to F_2CO + FSNO.

To verify this assumption, IR frequencies of $CF_2{=}NSO_2F$ (e) were calculated (Table S1, Supporting Information). For its C=N stretching vibration a strong IR band is predicted at 1790 cm^{-1} and a ^{15}N-isotopic shift of 21.1 cm^{-1}. An as yet unassigned broad band located at 1768.3 cm^{-1} and observed among the ArF laser photolysis products of $CF_3SO_2N_3$ (a)

dx.doi.org/10.1021/jp506243s | J. Phys. Chem. A XXXX, XXX, XXX−XXX

Table 1. Observed and Calculated IR Wavenumber (ν_i) and ^{15}N Isotopic Shifts ($\Delta\nu(^{14/15}N)$) of CF_3SO_2N (b)

observed[a]			calculated[b]			
Ne matrix	Ar matrix					
ν_i	ν_i	$\Delta\nu(^{14/15}N)$[c]	ν_i (^1A)[d]	ν_i ($^3A''$)[e]	$\Delta\nu(^{14/15}N)$[e]	assignment[f]
1389.8 s	1387.4 s	n.r.	1419 (193)	1383 (194)	0.0	ν_{12}, SO_2 asym stretch
1232.1 s	1231.7 s	n.r.	1232 (195)	1219 (216)	0.0	ν_1, CF_3 asym stretch
1227.6 s	1225.8 s	n.r.	1201 (251)	1211 (194)	0.0	ν_{13}, CF_3 asym stretch
1179.8 w	1171.8 w	n.r.	1159 (118)	1197 (29)	0.0	ν_2, SO_2 sym stretch
1117.2 s	1115.5 s	n.r.	1018 (196)	1096 (281)	0.0	ν_3, CF_3 sym stretch
			760 (6)	763 (0.8)	0.6	ν_4, CF_3 deform.
723.2 w	720.9 w	8.2	990 (6)	706 (29)	9.8	ν_5, SN stretch
			560 (65)	549 (<1)	0.5	ν_6, CF_3 deform.
	553.2 w	n.r.	550 (1)	548 (25)	2.4	ν_{14}, CF_3 deform.
	539.2 m	0.5	544 (51)	532 (73)	0.3	ν_7, SO_2 deform.
	478.7 w	2.5	442 (22)	463 (31)	4.2	ν_8
	380.0 vw	n.r.	387 (5)	362 (6)	0.8	ν_{15}
			338 (<1)	300 (<1)	0.4	ν_9
	290.5 vw	3.6	296 (1)	269 (2)	3.7	ν_{16}
			279 (2)	265 (3)	1.9	ν_{10}
			185 (2)	180 (2)	0.0	ν_{17}
			180 (3)	168 (2)	2.9	ν_{11}
			41 (<1)	37 (<1)	0.3	ν_{18}

[a]Experimentally observed band positions (cm^{-1}) of most intensive matrix sites, band intensities: s, strong; medium strong, m; w, weak; vw, very weak. [b]B3LYP/6-311+G(3df) calculated IR frequencies (cm^{-1}) and absolute intensities (km mol^{-1}) in parentheses. [c]n.r. = not resolved. [d]Singlet CF_3SO_2N (^1A). [e]Triplet CF_3SO_2N ($^3A''$). [f]Tentative assignments were made according to calculated displacement vectors for triplet CF_3SO_2N ($^3A''$).

Table 2. Observed and Calculated IR Wavenumber (cm^{-1}) of CF_3NSO_2 (c)

Ne-matrix[a] photolysis	Ar-matrix[b] photolysis	Ar-matrix[b] pyrolysis	calculated[c]
1420.5 s	1416.9 s	1413.1 s	1421 (204)
1319.1 s	1316.6 s	1313.6 s	1332 (470)
1248.4 s	1244.9 s	1243.8 s	1230 (351)
1219.2 s	1218.5 s	1213.1 s	1192 (236)
1196.1 s	1194.2 s	1196.3 s	1163 (318)
1047.7 m	1047.1 m	1045.4 m	1050 (142)
	584.9 w	585.3 w	581 (27)
	466.0 w	471.9 w	470 (13)
	410.5 vw	406.0 vw	403 (11)

[a]Band positions in the Ne matrix obtained by photolysis of $CF_3SO_2N_3$, band intensities: s, strong; medium strong; m, w, weak; vw, very weak. [b]Band positions in the Ar matrix obtained by photolysis and flash pyrolysis[26] of $CF_3SO_2N_3$, respectively. [c]B3LYP/6-311+G(3df) calculated IR frequencies (>400 cm^{-1}) and absolute intensities (>10 km mol^{-1}) in parentheses.

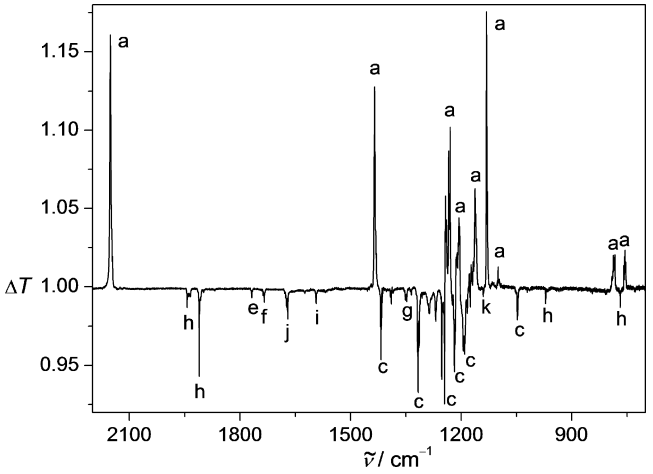

Figure 3. IR spectral changes (transmission T) in the region 2200–700 cm^{-1} obtained upon high-pressure mercury lamp irradiation (λ > 225 nm, 60 min) of Ar-matrix isolated $CF_3SO_2N_3$ (a) at 16 K. Assigned photolysis-products: CF_3NSO_2 (c), CF_2NSO_2F (e), CF_2NF (f), SO_2 (g), F_2CO (h), CF_3NO (i), FSNO (j), and SO (k).

(Figure 2A,B) can tentatively be assigned to $CF_2{=}NSO_2F$ (e). Its band position and the observed ^{15}N-isotopic shift (19.7 cm^{-1}) are close to the predictions (1790 cm^{-1}, 21.1 cm^{-1}), and close to the corresponding data of $CF_2{=}NF$ (f, 1737.2 cm^{-1}, $\Delta\nu(^{14/15}N)$ = 16.7 cm^{-1}). This assignment is further supported by the presence of an additional weak band at 1454.4 cm^{-1} (Figure 2A), which likely can be attributed to the asymmetric SO_2 stretch of the carrier (e). Its ^{15}N-isotope shift is not resolved (Figure 2B), which is consistent with DFT-calculated results for $CF_2{=}NSO_2F$ (1471 cm^{-1}, $\Delta\nu(^{14/15}N)$ = 0.1 cm^{-1}). However, due to the overlap with spectra of other species in the highly congested region of 1300–1100 cm^{-1} (Figure 3), no further bands could be convincingly attributed to this novel species. It is worthwhile to note that both these bands did not appear in Figures 2C,D and 3, where intermediate (e) is expected to photodecompose into F_2CO (h) + FSNO (j).

The triplet ground state nature of CF_3SO_2N (b) and also the intervention of CF_3N radical (l) as the precursor of CF_2NF (f), have been confirmed by their EPR spectra obtained from the ArF laser photolysis products of Ar-matrix isolated $CF_3SO_2N_3$ (a) at 6 K and depicted in Figure 4.

Obviously, there are two sets of nitrene signals (Figure 4A). The weaker one centered at 8680 G was found to have the zero-field splitting parameters (ZFSP) $|D/hc|$ = 1.741 cm^{-1} and $|E/hc|$ = 0 cm^{-1} (Figure 4C), and corresponded to known triplet CF_3N ($|D/hc|$ = 1.736 cm^{-1}).[44] Probably because of its

dx.doi.org/10.1021/jp506243s | J. Phys. Chem. A XXXX, XXX, XXX–XXX

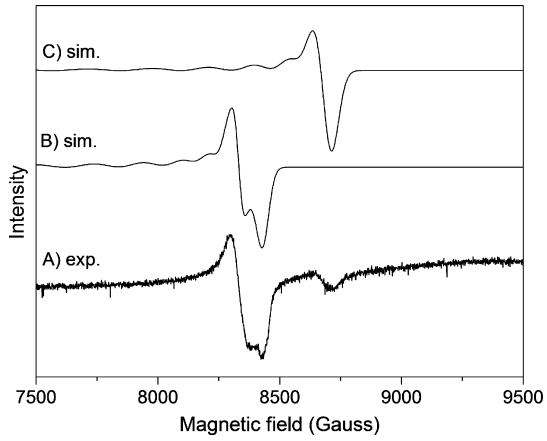

Figure 4. (A) Experimental EPR spectrum of the ArF laser photolysis products of Ar matrix isolated $CF_3SO_2N_3$. (B) and (C) EPR spectra (g = 2.003, ν = 9.60614 GHz) simulated by using zero-field splitting parameters of $|D/hc|$ = 1.595 cm^{-1}, $|E/hc|$ = 0.0018 cm^{-1} and $|D/hc|$ = 1.741 cm^{-1}, $|E/hc|$ = 0.0 cm^{-1}, respectively.

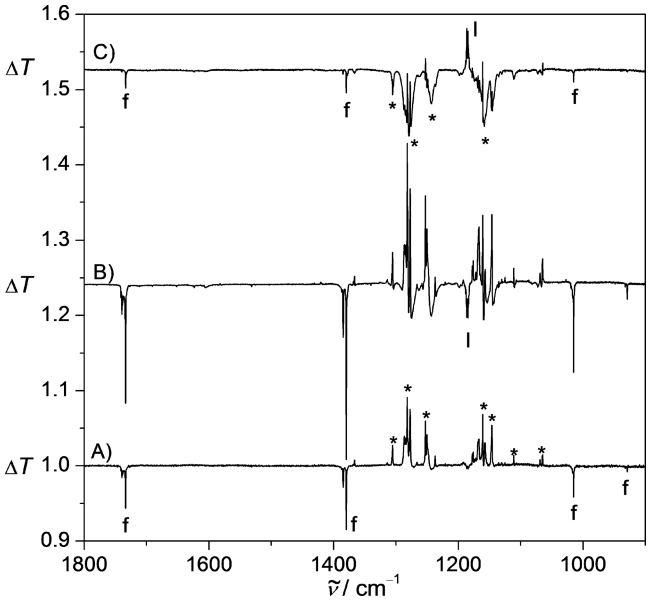

Figure 5. IR spectral changes (transmission T) in the region 1800–900 cm^{-1} obtained upon (A) ArF laser photolysis (λ = 193 nm, 7 min) of Ar-matrix isolated CF_3N_3 at 16 K, (B) further UV irradiation (λ = 254 nm, 20 min), and (C) further near UV–visible irradiation ($\lambda \geq$ 335 nm, 10 min). Bands of CF_3N_3 are marked by asterisks, and bands of CF_2=NF and CF_3N ($^3A_2$) are indicated by f and l, respectively.

low abundance, this transient species was not detected directly in the complex IR spectra of the photolysis products of $CF_3SO_2N_3$, and only its rearrangement product CF_2=NF (f) was observed (Figure 2). For the much stronger EPR signal centered at 8340 G the ZFSP of $|D/hc|$ = 1.595 cm^{-1} and $|E/hc|$ = 0.0018 cm^{-1} are determined (Figure 4B). It corresponds to triplet CF_3SO_2N ($^3A''$). The ZFSP are close to those of other triplet sulfonylnitrenes such as FSO_2N ($|D/hc|$ = 1.620 cm^{-1}, $|E/hc|$ = 0.0055 cm^{-1})[23] and $PhSO_2N$ ($|D/hc|$ = 1.569 cm^{-1}, $|E/hc|$ = 0 cm^{-1}).[20] According to integrated intensities of the two EPR signals, a ratio of CF_3SO_2N:$CF_3N \approx$ 23(3):1 can be estimated. It is assumed that CF_3N formed by photodecomposition of the azide immediately converts into CF_2=NF (f) under the irradiation conditions.

Triplet (trifluoromethyl)nitrene, CF_3N ($^3A_2$), has previously been generated in solid Ar matrices at 14 K from CF_3N_3 by using a "pen lamp" (λ = 254 nm).[44] The low concentration allowed its detection only due to an intensive UV transition at λ_{max} = 354 nm, from which two vibrational progressions of about 1160 and 500 cm^{-1} were derived for the excited ^3E state.[44] The absence of any vibrational data for the ground state ($^3A_2$) prompted us to revisit the photolysis of matrix-isolated CF_3N_3.

When Ar-matrix isolated CF_3N_3 was subjected to ArF laser (λ = 193 nm) irradiation, CF_2=NF (f) was observed as the main product and a few additional very weak new IR bands appeared (Figure 5A). Attempts to increase their intensities with prolonged photolysis time failed. The imine CF_2=NF was also formed by photolysis of CF_3N_3 using a low-pressure mercury lamp (λ = 254 nm), at which two new bands arose in the C–F stretching region at 1186.4 and 1184.3 cm^{-1} (Figure 5B). These bands completely disappeared after subsequent irradiation using filtered light of λ > 335 nm with concomitant formation of the azide precursor and of traces of CF_2=NF (Figure 5C). This observation is in accord with the expected behavior of triplet CF_3N ($^3A_2$) and with its reported UV transition at λ_{max} = 354 nm.[44] The partial re-formation of CF_3N_3 from CF_3N ($^3A_2$) and N_2 as well as the CF_3N to CF_2=NF rearrangement imply the transient formation of singlet excited CF_3N upon the irradiation, likely through intersystem crossing from a triplet excited state. The observed band position of triplet CF_3N ($^3A_2$) of 1184.3 cm^{-1} and its matrix site at 1186.4 cm^{-1} are slightly higher in frequency than the corresponding C–F stretching vibration in the electronically excited ^3E state (1160 cm^{-1}).[44] DFT calculations support this assignment and predict a rather strong (IR intensity: 673 km mol^{-1}) degenerate asymmetric CF_3 stretching vibration of CF_3N ($^3A_2$) at 1153 cm^{-1} (Table S4, Supporting Information). In contrast, the symmetric CF_3 stretch calculated at 1233 cm^{-1} revealed a much lower IR intensity (132 km mol^{-1}). It could not be assigned due to interferences with the strong IR bands of the azide precursor in this region.

Quantum Chemical Calculations. Molecular structures of CF_3SO_2N and its isomers were fully optimized by using different theoretical methods (B3LYP, BP86, MPW1PW91, and CBS-QB3). Calculated key structural parameters are shown in Figure 6, and their relative energies are collected in Table 3.

Generally, all applied theoretical methods provide consistent results (Table 3). The singlet–triplet gap of CF_3SO_2N was calculated at the most accurate CBS-QB3 level of theory to 29.5 kJ mol^{-1}. This energy gap is similar to that of 2-$NpSO_2N$ (33 kJ mol^{-1}, CBS-QB3).[21] For 2-$NpSO_2N$ the lowest excited singlet state adopts a closed-shell configuration, which was attributed to an effective intramolecular oxygen–nitrogen interaction in the excited singlet state. Such an intramolecular interaction is also indicated by the molecular structure of CF_3SO_2N (^1A), which reveals a short O–N distance of 1.800 Å and a small OSN angle of 72.2° (triplet: 107.9°, B3LYP/6-311+G(3df)). Similar intramolecular O–N interactions have been predicted for related singlet α-oxo nitrenes such as RC(O)N[5,6] and $R_2P(O)N$.[45,46]

The calculated S–N bonds in CF_3SO_2N are 1.886 and 1.878 Å for the triplet and singlet states, respectively. Both are much longer than those calculated for the thermally persistent FSO_2N, 1.670 (triplet) and 1.535 Å (singlet).[25] The weak $F_3C^{\delta+}$–$S^{\delta+}$ bond in CF_3SO_2N is most likely responsible for its facile fragmentation into O_2SN and CF_3 during the flash

dx.doi.org/10.1021/jp506243s | J. Phys. Chem. A XXXX, XXX, XXX–XXX

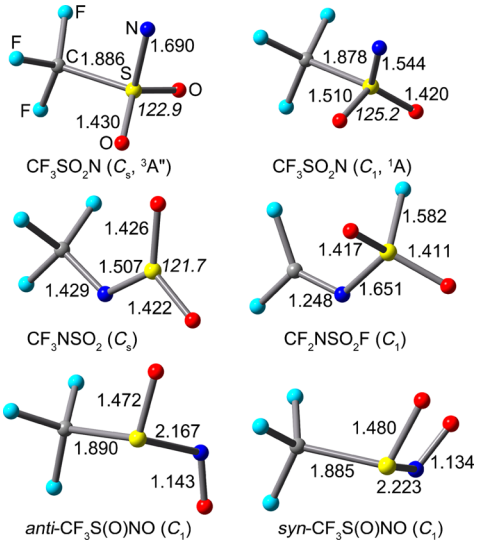

Figure 6. Optimized structures of CF_3SO_2N and its isomers at the B3LYP/6-311+G(3df) level of theory. Selected bond lengths and angles (italics) are given in (Å) and (deg), respectively, and the molecular symmetry is indicated in parentheses.

Table 3. Calculated Relative Energies (kJ mol^{-1}) of CF_3SO_2N Isomers Obtained with Different Theoretical Methods

	B3LYP[a]	BP86[a]	MPW1PW91[a]	CBS-QB3
CF_3SO_2N ($^3A''$)	−58.9	−28.8	−66.5	−29.5
CF_3SO_2N (^1A)	0	0	0	0
$CF_3{=}NSO_2$	−332.8	−314.0	−336.4	−322.2
syn-$CF_3S(O)NO$	−190.5	−193.7	−168.0	−161.7
anti-$CF_3S(O)NO$	−171.1	−173.8	−148.0	−138.5
$CF_2{=}NSO_2F$	−378.6	−354.3	−383.3	−370.1

[a]The 6-311+G(3df) basis set was used.

pyrolysis of $CF_3SO_2N_3$.[26] Note that this decomposition route is spin-allowed in both the triplet ground state and the singlet excited state of the nitrene. In addition, a weak C−S bond in the singlet state also facilitates a Curtius-type rearrangement of CF_3SO_2N to CF_3NSO_2. The corresponding moderate activation barrier of 107.2 kJ mol^{-1} obtained at the B3LYP/6-311+G(3df) level of theory is lower than that required for the rearrangement to $CF_3S(O)NO$ (123.6 kJ mol^{-1}), which probably explains the absence of $CF_3S(O)NO$ during the thermal decomposition of the azide.

Optimized structures of *syn*- and *anti*-$CF_3S(O)NO$ have previously been reported,[47] where it has been suggested that these intermediates may play an important role in the oxidation of CF_3S by NO_2. Our computed structures for these two conformers are consistent with the previous results. Their extremely long S−N bond lengths (*syn*, 2.223 Å; *anti*, 2.167 Å) suggests a facile dissociation into CF_3SO and NO radicals, which in solid matrices is probably prevented by the matrix cage. In fact, the N−O stretching frequency observed for $CF_3S(O)NO$ (1831.9 cm^{-1}) is fairly close to that obtained for free NO in an argon matrix (1874.5 cm^{-1}).[48]

The suggested rearrangement from CF_3NSO_2 to CF_2NSO_2F has also been studied computationally and a four-membered ring transition state for the fluorine shift was located. Its barrier of 131.2 kJ mol^{-1} likely rules out the formation of CF_2NSO_2F by flash pyrolysis of $CF_3SO_2N_3$, whereas the large excess of energy used in the photolysis experiment enables the further rearrangement of CF_3NSO_2 to CF_2NSO_2F.

CONCLUSIONS

The photochemistry of $CF_3SO_2N_3$ in solid noble gas matrices has been studied. In contrast to the previously reported straightforward thermal decomposition of $CF_3SO_2N_3$,[26] its photodecomposition is more complex and furnished a variety of secondary products (Figure 7). It enabled the first

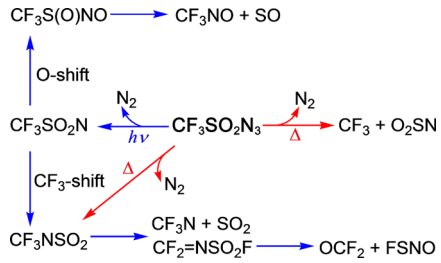

Figure 7. Experimentally observed photodecomposition (blue line) and thermal (red line) decomposition pathways for $CF_3SO_2N_3$.

identification of several novel intermediates like CF_3SO_2N ($^3A''$), $CF_3S(O)NO$, CF_2NSO_2F, and FSNO. Initially, a singlet nitrene intermediate CF_3SO_2N (^1A) is formed from the azide by elimination of N_2 upon UV irradiation. The singlet nitrene either may relax to the triplet ground state ($^3A''$) or is subjected to a Curtius-type rearrangement. Both an "oxygen shift" and migration of the CF_3 group to yield $CF_3S(O)NO$ and CF_3NSO_2, respectively, are observed upon photolysis in solid noble gas matrices. Photofragmentation of $CF_3S(O)NO$ yields CF_3NO and SO, whereas CF_3NSO_2 may dissociate into CF_3N + SO_2. Also OCF_2 + FSNO and CF_2NSO_2F have finally been detected among the photolysis products of $CF_3SO_2N_3$.

The present matrix isolation study on $CF_3SO_2N_3$ will contribute to the understanding of the fundamental chemistry of sulfonyl azides and helps to understand their complicated photochemistry in solution, which for a long time have impaired the broader application of sulfonyl azides as the nitrene precursor.[7−17] The distinct photodecomposition and thermal decomposition of the sulfonyl azides $CF_3SO_2N_3$[26] and FSO_2N_3[23,25] and the surprisingly different reactivity of the corresponding sulfonylnitrenes certainly demand further systematic theoretical studies.

ASSOCIATED CONTENT

Supporting Information

Calculated IR and UV−vis spectroscopic data, energies, and atomic coordinates for all species discussed in the paper. Complete ref 39. This material is available free of charge via the Internet at http://pubs.acs.org.

AUTHOR INFORMATION

Corresponding Authors

*X. Q. Zeng: e-mail, zeng@suda.edu.cn; phone, +86 512 65883583.

*H. Beckers: e-mail, beckers@uni-wuppertal.de; phone, +49 202 4392504.

Notes

The authors declare no competing financial interest.

dx.doi.org/10.1021/jp506243s | J. Phys. Chem. A XXXX, XXX, XXX−XXX

■ ACKNOWLEDGMENTS

This work was supported by the National Natural Science Foundation of China (21372173) and the Deutsche Forschungsgemeinschaft. X.Z. gratefully acknowledges Prof. H. Willner for a research stay in Wuppertal. We are indebted to Prof. T. Benter for making use of the ArF laser and to Prof. R. Sheridan for sharing unpublished spectra.

■ REFERENCES

(1) Kim, J. Y.; Park, S. H.; Ryu, J.; Cho, S. H.; Kim, S. H.; Chang, S. Rhodium-Catalyzed Intermolecular Amidation of Arenes with Sulfonyl Azides via Chelation-Assisted C−H Bond Activation. *J. Am. Chem. Soc.* **2012**, *134*, 9110−9113.

(2) Katritzky, A. R.; Khatib, M. E.; Bol'shakov, O.; Khelashvili, L.; Steel, P. J. Benzotriazol-1-yl-sulfonyl Azide for Diazotransfer and Preparation of Azidoacylbenzotriazoles. *J. Org. Chem.* **2010**, *75*, 6532−6539.

(3) Cano, I.; Nicasio, M. C.; Pérez, P. J. Copper(I) Complexes as Catalysts for the Synthesis of N-sulfonyl-1,2,3-triazoles from N-sulfonylazides and Alkynes. *Org. Biomol. Chem.* **2010**, *8*, 536−538.

(4) Raushel, J.; Pitram, S. M.; Fokin, V. V. Efficient Synthesis of Sulfonyl Azides from Sulfonamides. *Org. Lett.* **2008**, *10*, 3385−3388.

(5) Vyas, S.; Kubicki, J.; Luk, H. L.; Zhang, Y.; Gritsan, N. P.; Hadad, C. M.; Platz, M. S. An Ultrafast Time-resolved Infrared and UV−vis Spectroscopic and Computational Study of the Photochemistry of Acyl Azides. *J. Phys. Org. Chem.* **2012**, *25*, 693−703.

(6) Kubicki, J.; Zhang, Y.; Vyas, S.; Burdzinski, G.; Luk, H. L.; Wang, J.; Xue, J.; Peng, H.-L.; Pritchina, E. A.; Sliwa, M.; et al. Photochemistry of 2-Naphthoyl Azide. An Ultrafast Time-resolved UV-vis and IR Spectroscopic and Computational Study. *J. Am. Chem. Soc.* **2011**, *133*, 9751−9761.

(7) Sheridan, R. S.; Rempala, P. *Books of Abstracts*, 217th ACS National Meeting, Anaheim, CA; American Chemical Society: Washington, DC, 1999; ORGN-287.

(8) Desikan, V.; Liu, Y.; Toscano, J. P.; Jenks, W. S. Photochemistry of *N*-Acetyl-, *N*-Trifluoroacetyl-, *N*- Mesyl-, and *N*-Tosyldibenzothiophene Sulfilimines. *J. Org. Chem.* **2008**, *73*, 4398−4414.

(9) Garay, J.-C.; Maloney, V.; Marlow, M.; Small, P. Spectroscopy and Kinetics of Triplet 4-Methylbenzenesulfonylnitrene. *J. Phys. Chem.* **1996**, *100*, 5788−5793.

(10) Abramovitch, R. A.; Sutherland, R. G. Recent Aspects of the Chemistry of Sulphonyl Nitrenes. *Top. Curr. Chem.* **1970**, *16*, 1−33.

(11) Abramovitch, R. A.; Davis, B. A. Preparation and Properties of Imido Intermediates (Imidogens). *Chem. Rev.* **1964**, *64*, 149−185.

(12) Abramovitch, R. A.; Holcomb, W. D.; Wake, S. The Decomposition of *β*-Phenethylsulfonyl Azides. Solution Chemistry and Flash Vacuum Pyrolysis. *J. Am. Chem. Soc.* **1981**, *103*, 1525−1533.

(13) Abramovitch, R. A.; Knaus, G. N.; Uma, V. Aromatic Substitution by Sulfonyl Nitrenes. Singlet or Triplet Reactive Intermediates. *J. Am. Chem. Soc.* **1969**, *91*, 7532−7533.

(14) Abramovitch, R. A.; Azogu, C. I.; McMaster, I. T. Intramolecular Cyclizations of Sulfonyl Nitrenes. *J. Am. Chem. Soc.* **1969**, *91*, 1219−1220.

(15) Breslow, D. S.; Sloan, M.; Newburg, N. R.; Renfrow, W. B. Thermal Reactions of Sulfonyl Azides. *J. Am. Chem. Soc.* **1969**, *91*, 2273−2279.

(16) Lwowski, W.; Scheiffele, E. Curtius and Lossen Rearrangements. I. The Benzenesulfonyl System. *J. Am. Chem. Soc.* **1965**, *87*, 4359−4365.

(17) Abramovitch, R. A.; Holcomb, W. D. Curtius-type Rearrangement of a Sulphonyl Azide. *Chem. Commun.* **1969**, 1298−1299.

(18) Moriarty, R. M.; Rahman, M.; King, G. J. Organic Nitrenes in Single Crystals. Observation of Hyperfine Structure in the Electron Spin Resonance. *J. Am. Chem. Soc.* **1966**, *88*, 842−843.

(19) Garay, J.-C.; Maloney, V.; Marlow, M.; Small, P. Spectroscopy and Kinetics of Triplet 4-Methylbenzenesulfonylnitrene. *J. Phys. Chem.* **1996**, *100*, 5788−5793.

(20) Smolinsky, G.; Wasserman, E.; Yager, W. A. The E.P.R. of Ground State Triplet Nitrenes. *J. Am. Chem. Soc.* **1962**, *84*, 3220−3221.

(21) Kubicki, J.; Luk, H. L.; Zhang, Y.; Vyas, S.; Peng, H.-L.; Hadad, C. M.; Platz, M. S. Direct Observation of a Sulfonyl Azide Excited State and Its Decay Processes by Ultrafast Time-Resolved IR Spectroscopy. *J. Am. Chem. Soc.* **2012**, *134*, 7036−7044.

(22) Kubicki, J.; Zhang, Y.; Xue, J.; Luk, H. L.; Platz, M. S. Ultrafast Time Resolved Studies of the Photochemistry of Acyl and Sulfonyl Azides. *Phys. Chem. Chem. Phys.* **2012**, *14*, 10377−10390.

(23) Zeng, X. Q.; Beckers, H.; Neuhaus, P.; Grote, D.; Sander, W. Elusive Fluoro Sulfinyl Nitrite, FS(O)NO, Produced by Photolysis of Matrix-isolated $FS(O)_2N$. *Z. Anorg. Allg. Chem.* **2012**, *638*, 526−533.

(24) Zeng, X. Q.; Beckers, H.; Willner, H.; Neuhaus, P.; Grote, D.; Sander, W. Difluorophosphoryl Nitrene $F_2P(O)N$: Matrix Isolation and Unexpected Rearrangement to F_2PNO. *Chem. −Eur. J.* **2009**, *15*, 13466−13473.

(25) Zeng, X. Q.; Beckers, H.; Willner, H. Thermally Persistent Fluorosulfonyl Nitrene and Unexpected Formation of the Fluorosulfonyl Radical. *J. Am. Chem. Soc.* **2013**, *135*, 2096−2099.

(26) Zeng, X. Q.; Beckers, H.; Willner, H. The Iminyl Radical O_2SN. *Angew. Chem., Int. Ed.* **2013**, *52*, 7981−7984.

(27) Shainyan, B. A.; Tolstikova, L. L. Trifluoromethanesulfonamides and Related Compounds. *Chem. Rev.* **2013**, *113*, 699−733 and references therein..

(28) Zeng, X. Q.; Gerken, M.; Beckers, H.; Willner, H. Anomeric Effects in Sulfonyl Compounds: An Experimental and Computational Study of Fluorosulfonyl Azide, FSO_2N_3, and Trifluoromethylsulfonyl Azide, $CF_3SO_2N_3$. *J. Phys. Chem. A* **2010**, *114*, 7624−7630.

(29) Schnöckel, H. G.; Willner, H. In *Infrared and Raman Spectroscopy, Methods and Applications*; Schrader, B., Ed.; VCH: Weinheim, 1994.

(30) Griffin, M.; Muys, A.; Noble, C.; Wang, D.; Eldershaw, C.; Gates, K. E.; Burrage, K.; Hanson, G. R. XSophe, a Computer Simulation Software Suite for the Analysis of Electron Paramagnetic Resonance Spectra. *Mol. Phys. Rep.* **1999**, *26*, 60−84.

(31) Becke, A. D. Density-Functional Thermochemistry. III. The Role of Exact Exchange. *J. Chem. Phys.* **1993**, *98*, 5648−5652.

(32) Adamo, C.; Barone, V. Exchange Functionals with Improved Long-range Behavior and Adiabatic Connection Methods without Adjustable Parameters: The mPW and mPW1PW Models. *J. Chem. Phys.* **1998**, *108*, 664−675.

(33) Perdew, J. P. Density-functional Approximation for the Correlation Energy of the Inhomogeneous Electron Gas. *Phys. Rev. B* **1986**, *33*, 8822−8824.

(34) Montgomery, J. A., Jr.; Frisch, M. J.; Ochterski, J. W.; Petersson, G. A. A Complete Basis Set Model Chemistry. VII. Use of the Minimum Population Localization Method. *J. Chem. Phys.* **2000**, *112*, 6532−6542.

(35) Stratmann, R. E.; Scuseria, G. E.; Frisch, M. J. An Efficient Implementation of Time-dependent Density-functional Theory for the Calculation of Excitation Energies of Large Molecules. *J. Chem. Phys.* **1998**, *109*, 8218−8224.

(36) Foresman, J. B.; Head-Gordon, M.; Pople, J. A.; Frisch, M. J. Toward a Systematic Molecular Orbital Theory for Excited States. *J. Phys. Chem.* **1992**, *96*, 135−149.

(37) Fukui, K. The Path of Chemical Reactions - the IRC Approach. *Acc. Chem. Res.* **1981**, *14*, 363−368.

(38) Hratchian, H. P.; Schlegel, H. B. Using Hessian Updating To Increase the Efficiency of a Hessian Based Predictor-Corrector Reaction Path Following Method. *J. Chem. Theory Comput.* **2005**, *1*, 61−69.

(39) Frisch, M. J.; Trucks, G. W.; Schlegel, H. B.; Scuseria, G. E.; Robb, M. A.; Cheeseman, J. R.; Montgomery, J. A. Jr.; Vreven, T.; Kudin, K. N.; Burant, J. C.; et al. *Gaussian 03*, revision D.01; Gaussian, Inc.: Wallingford, CT, 2003.

(40) Jacobs, J.; Jülicher, B.; Schatte, G.; Willner, H.; Mack, H.-G. CFNO-Isomere − Theoretische und Experimentelle Studien. *Chem. Ber.* **1993**, *126*, 2167−2176.

(41) Demuth, R.; Bürger, H.; Pawelke, G.; Willner, H. Gas- Und Matrix-IR-Spektren von $CF_3{}^{15}NO$. *Spectrochim. Acta* **1978**, *34*, 113−114.
(42) Christen, D.; Oberhammer, H.; Hammaker, R. M.; Chang, S.-C.; DesMarteau, D. D. Structure of Perfluoromethanimine by Microwave, Infrared, and Raman spectroscopy, Electron Diffraction, and Ab Initio Methods. *J. Am. Chem. Soc.* **1982**, *104*, 6186−6190.
(43) Mason, J. Trifluoromethyl Thionitrite. *J. Chem. Soc.* **1969**, 1587−1592.
(44) Gritsan, N. P.; Likhotvorik, I.; Zhu, Z. D.; Platz, M. S. Observation of Perfluoromethylnitrene in Cryogenic Matrixes. *J. Phys. Chem. A* **2001**, *105*, 3039−3041.
(45) Vyas, S.; Muthukrishnan, S.; Kubicki, J.; McCulla, R. D.; Burdzinski, G.; Sliwa, M.; Platz, M. S.; Hadad, C. M. Ultrafast Spectroscopy and Computational Study of the Photochemistry of Diphenylphosphoryl Azide: Direct Spectroscopic Observation of a Singlet Phosphorylnitrene. *J. Am. Chem. Soc.* **2010**, *132*, 16796−16804.
(46) McCulla, R. D.; Gohar, G. A.; Hadad, C. M.; Platz, M. S. Computational Study of the Curtius-like Rearrangements of Phosphoryl, Phosphinyl, and Phosphinoyl Azides and Their Corresponding Nitrenes. *J. Org. Chem.* **2007**, *72*, 9426−9438.
(47) Lesar, A.; Kosmas, A. M. Theoretical Study on the Mechanism of the Reaction of CF_3S with NO_2. *J. Phys. Chem. A* **2010**, *114*, 1147−1152.
(48) Krim, L.; Lacome, N. The NO Dimer, ^{14}N and ^{15}N Isotopomers Isolated in Argon Matrix: A Near-, Mid-, and Far-Infrared Study. *J. Phys. Chem. A* **1998**, *102*, 2289−2296.